Calibration of liquid argon and neon detectors with ^{83}Kr$^{\rm m}$

W. H. Lippincott,[1] S. B. Cahn,[1] D. Gastler,[2] L. W. Kastens,[1] E. Kearns,[2] D. N. McKinsey,[1, *] and J. A. Nikkel[1]

[1]*Department of Physics, Yale University, New Haven, CT 06511*
[2]*Department of Physics, Boston University, Boston, MA 02215*
(Dated: November 28, 2009)

We report results from tests of ^{83}Kr$^{\rm m}$ as a calibration source in liquid argon and liquid neon. ^{83}Kr$^{\rm m}$ atoms are produced in the decay of ^{83}Rb, and a clear ^{83}Kr$^{\rm m}$ scintillation peak at 41.5 keV appears in both liquids when filling our detector through a piece of zeolite coated with ^{83}Rb. Based on this scintillation peak, we observe 6.0 photoelectrons/keV in liquid argon with a resolution of 6% (σ/E) and 3.0 photoelectrons/keV in liquid neon with a resolution of 19% (σ/E). The observed peak subsequently decays with the appropriate half-life after stopping the fill, and we find evidence that the spatial location of ^{83}Kr$^{\rm m}$ atoms in the chamber can be resolved. ^{83}Kr$^{\rm m}$ will be a useful calibration source for liquid argon and neon dark matter and solar neutrino detectors.

PACS numbers:

I. INTRODUCTION

Liquefied nobles gases are now being widely used as targets in low background searches, particularly in direct dark matter searches where a weakly interacting massive particle (WIMP) may scatter elastically with a nucleus to produce a nuclear recoil in the liquid. Several WIMP-nucleon cross-section limits have been set in recent years using liquid argon and xenon, and several larger, more sensitive argon and xenon detectors are currently under construction [1–4]. Liquid neon is another target attracting interest, having been proposed as a potential target for pp-solar neutrinos in addition to dark matter [5, 6]. In particular, the MiniCLEAN detector which will be deployed at SNOLAB in the Creighton mine in Sudbury, Ontario will run in both liquid argon and liquid neon phases [7].

Because the expected dark matter signal has energies in the tens of keV and drops exponentially with increasing energy, a dark matter detector must be calibrated at low energy to precisely determine its energy threshold and ultimate WIMP sensitivity. Low energy calibrations are also important for a liquid neon pp neutrino detector because any uncertainty in the energy scale produces a systematic error in the observed neutrino energy spectrum and flux. As liquid noble gas detectors get larger, self-shielding will render it increasingly difficult to illuminate the central volume of the liquid with external gamma rays, particularly at low energies. Therefore, a low-energy radioactive source that can be distributed throughout the detector volume is highly desirable for calibrating the new generation of liquid noble gas detectors. One example of such a calibration was the introduction of activated xenon isotopes into the XENON10 detector. A sample of xenon was irradiated at Yale University to produce ^{129}Xe$^{\rm m}$ and ^{131}Xe$^{\rm m}$, which emit 236 keV and 164 keV gamma rays with half-lives of 8.9

and 11.8 days, respectively. This sample was shipped to Gran Sasso National Laboratory in Italy and introduced into the detector to provide a uniform energy calibration [8]. While this calibration was successful, the energies of these isotopes are higher than those expected from a WIMP signal and their relatively long half-lives limit the frequency of deployment.

An alternative is the use of ^{83}Kr$^{\rm m}$, which is used as a diagnostic tool for studying the beta decay of tritium and has been proposed for use with the KATRIN detector [9]. ^{83}Kr$^{\rm m}$ is produced in the decay of ^{83}Rb, which has a half-life of 86.2 days. In turn, the ^{83}Kr$^{\rm m}$ decays with a half-life of (1.83 ± 0.02) hours, emitting 32.1 keV and 9.4 keV conversion electrons (see Fig. 1) [10–12]. As a noble gas, ^{83}Kr$^{\rm m}$ is easily introduced into noble liquid detectors without compromising the purity of the liquid, and it is not expected to create any long-lived radioisotopes. Recently, ^{83}Kr$^{\rm m}$ has been successfully used to calibrate liquid xenon detectors [13, 14]. Because argon and neon are liquids at temperatures below the freezing point of krypton, any ^{83}Kr$^{\rm m}$ atoms in the liquid could potentially freeze out on detector surfaces before decaying. This paper describes successful tests of ^{83}Kr$^{\rm m}$ as a calibration source in both liquid argon and liquid neon. While some ^{83}Kr$^{\rm m}$ atoms may be freezing out, enough reach the center of the liquid volume to provide a good energy calibration.

II. EXPERIMENTAL APPARATUS

A schematic of the apparatus used to perform these measurements at Yale is shown in Fig 2. Known as MicroCLEAN, the apparatus has been described in detail elsewhere [15]. The detector has an active volume of 3.14 liters viewed by two 200-mm-diameter Hamamatsu R5912-02MOD photomultiplier tubes (PMTs), which are specifically designed for use in cryogenic liquids. The active volume is defined by a polytetrafluoroethylene (PTFE) cylinder 200 mm in diameter and 100 mm in height, with two 3-mm-thick fused-silica windows at top
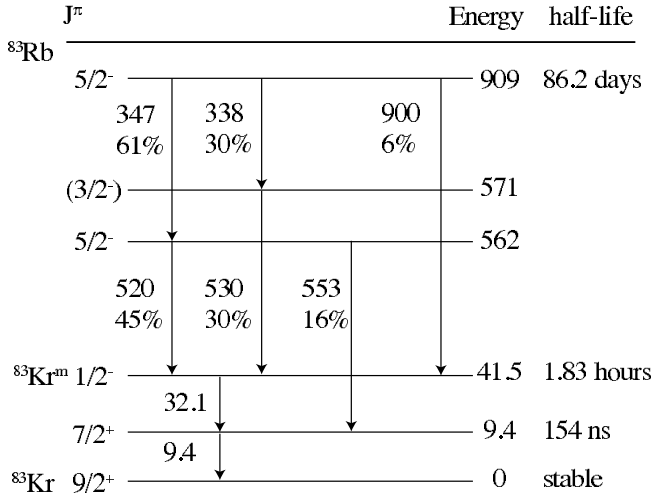
FIG. 1: Energy levels in keV of ^{83}Rb. 75% of the time, ^{83}Rb decays to ^{83}Kr^{m}, which in turns emits two conversion electrons at 32.1 and 9.4 keV. The half-life of ^{83}Kr^{m} to decay via the first electron to the $7/2^-$ state is 1.83 hours and the half-life for the subsequent decay to the stable $9/2^+$ state of ^{83}Kr is 154 ns.

and bottom. Both liquid argon and neon scintillate in the ultraviolet; therefore, all inner surfaces of the PTFE and windows are coated with (0.20 ± 0.01) mg/cm^2 of tetraphenyl butadiene (TPB) [16], which wavelength shifts the ultraviolet light to approximately 440 nm. The active volume, PTFE cylinder, windows and PMTs are all contained in a stainless steel vessel and immersed in the liquid. The stainless steel vessel is held within a large vacuum dewar, and the system is cooled by a pulse tube refrigerator connected to a copper liquefier. Argon or neon gas is passed through a getter for purification before entering the vacuum dewar, passing into the liquefier and dripping into the detector.
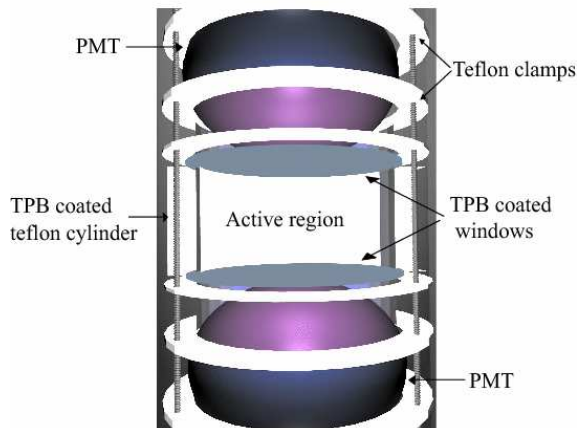

FIG. 2: (Color online) Schematic representation of the scintillation cell.

The ^{83}Rb source is the same source described in [13],

consisting of Rb-infused zeolite held in the bottom arm of a VCR cross. 700 nCi of ^{83}Rb were loaded into the zeolite trap in February, 2009. Given the ^{83}Rb half-life of 86.2 days, approximately 100 nCi remained in the trap when the tests described in this paper were performed in October and November, 2009.
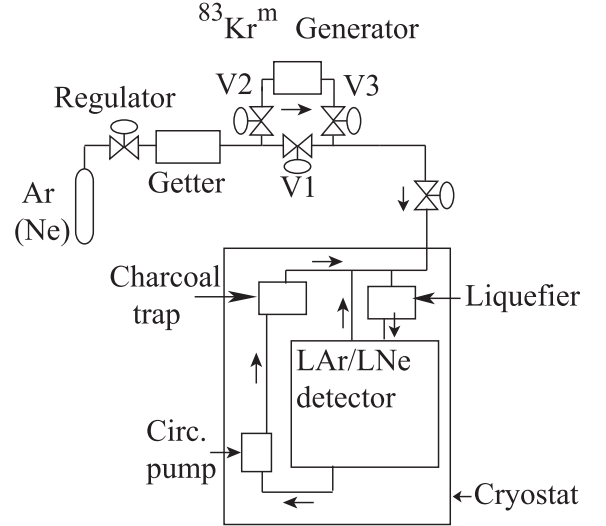

FIG. 3: The gas handling system for the ^{83}Kr^{m} runs. In active mode, valve V1 is closed while valves V2 and V3 are open. In passive mode, valves V1 and V3 are open while valve V2 is closed.

The gas handling system is shown in Fig. 3. The ^{83}Rb trap is connected to the gas inlet line just outside the vacuum dewar and the inlet gas can be diverted through the trap on its way into the detector. The ^{83}Rb remains attached to the zeolite, but the ^{83}Kr^{m} is free to escape with the flowing gas into the detector. There is an additional circulation loop inside the vacuum dewar. Liquid flows out of the bottom of the stainless steel vessel into a nearby VCR cross attached to a heater. The heater acts as a circulation pump by boiling the liquid, and the resulting gas then flows up a tube through a charcoal trap before reentering the top of the liquefier. This system was operated in two modes during the ^{83}Kr^{m} tests. In all cases, the heater/circulation pump was activated to ensure mixing of the liquid in the active region. In normal or "active" operation, argon or neon gas was flowed through the ^{83}Rb trap before entering the liquefier with the bypass valve, V1, closed. A second, "passive" mode was intended to test whether the trap needs to be actively in the circulation or filling path to introduce ^{83}Kr^{m} into the flow. In the passive mode, valve V2 between the getter and the trap was closed, valve V3 between the trap and the detector was open, and the bypass valve, V1, was open.

A. Data acquisition and processing

The data acquistion system consists of a 250 MHz, 12-bit CAEN V1720 waveform digitizer (WFD). Only the two PMT channels were recorded. Scintillation in argon and neon is produced in the decay of metastable molecules, and there are two decay channels with very different timing characteristics for both argon and neon, associated with the decay of singlet and triplet molecules. For electronic recoils in argon, roughly 30% of the light comes out promptly, while the rest is distributed in time with a lifetime of 1.5 μs [15]. For electronic recoils in neon, only 10% is emitted promptly, with the remainder distributed over at least 15 μs [17, 18]. Therefore, we collected different record lengths of data depending on the liquid under study; for argon, 16 μs of data were recorded for each event, while for neon, 64 μs were recorded. Figure 4 shows an example ^{83}Kr^{m} event in argon in which the two prompt components produced by the 32.1 and 9.4 keV electrons are highlighted. For the argon run, the trigger rate was recorded by a counter and monitored throughout the experiment. Unfortunately this counter was not available during neon running, and our knowledge of the trigger rate is therefore incomplete for the neon.

Single photoelectron spectra for the two PMTs are drawn from the tails of events as described in [15]. In neon, the gain of the PMTs drops by a factor of ~ 100 relative to argon, requiring the use of an additional amplifier. Also, the single photoelectron distribution of one of the PMTs becomes too dispersed to accurately measure a single value for the gain, and all light yield measurements are based on only one PMT. External calibration sources include 122 keV and 137 keV gamma rays from a ^{57}Co source, 356 keV gamma rays from a ^{133}Ba source, 511 keV gamma rays from a ^{22}Na source, and 662 keV gamma rays from a ^{137}Cs source.
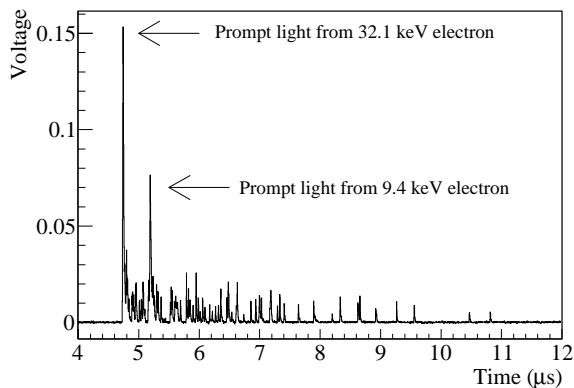

FIG. 4: Example of a ^{83}Kr^{m} event in liquid argon from a single PMT, digitized by the 12-bit CAEN WFD, sampling at 250 MHz. The 32.1 and 9.4 keV components of this particular ^{83}Kr^{m} event are highlighted.

The data processing, trace integration method and data cuts are similar to the methods described in [15]. In particular, we continue to use a cut designed to eliminate events that produce light in the windows or the glass of the PMTs by use of an asymmetry parameter, A. This parameter is defined as

$$A = \frac{S_T - S_B}{S_T + S_B}, \tag{1}$$

where S_T and S_B are the signal areas in the top and bottom PMTs, and the value of A gives a rough reconstruction of the z-position of an event in the detector. In analysis we require that $|A| < 0.4$. In the argon, 95% of events in the region around the observed ^{83}Kr^{m} peak pass all the cuts. Because there is less prompt scintillation light in neon than in argon and the PMT gains were greatly decreased, the trigger threshold was set extremely low for neon running, producing a large background of noise triggers. These noise triggers are largely eliminated by these cuts, and only 32% of all events in neon in the energy range around 41.5 keV pass the cuts.

III. DATA ANALYSIS AND RESULTS

A. Liquid Argon

We performed two ^{83}Kr^{m} runs in argon in normal mode by filling the cell through the ^{83}Kr^{m} generator for several hours before stopping the fill and watching the decay of the introduced ^{83}Kr^{m}. We also took several background runs to allow for a background subtraction. Running in this mode produced a clear peak in the argon, as shown in the top panel of Fig. 5. After performing a background subtraction, we fit the resulting peak to find an energy resolution of 8% (σ/E) at 41.5 keV, as shown in the lower panel of Fig. 5. We cannot report an energy resolution at 9.4 keV; due to the timing characteristics of scintillation in argon and neon, it is not possible to separate the light produced by the 9.4 keV electron from the late component of the 32.1 keV electron.

The light yield for the detector was (6.0 ± 0.2) photoelectrons (pe) per keV, or about 20% higher than that observed in [15]. We attribute the increase in light yield to the use of a thinner layer of TPB on the walls of the PTFE cell and to the substitution of a new PMT with a slightly higher quantum efficiency. The uncertainty is dominated by measurements of the gain in the top PMT. In terms of the total number of photoelectrons, the energy resolution of the peak was $1.3 \times \sqrt{<N_{pe}>}$. This analysis was repeated with a much tighter asymmetry cut and no change was observed in the energy resolution. As ^{83}Kr^{m} decays by emission of two electrons separated by a 154 ns half-life, a second analysis was performed to try and pick out a background-free collection of events by looking for the characteristic double peak structure (see Fig. 4). Again, no improvement in energy resolution was observed relative to the standard background subtracted analysis shown in Fig. 5.

Due to saturation of the PMTs, the voltage must be lowered to observe high energy recoils; at low voltage, the single photoelectron peak was not resolvable, although the $^{83}Kr^m$ peak remained clear. We took data using the four sources mentioned in the previous section during the steady state of a $^{83}Kr^m$ run. In each case, the $^{83}Kr^m$ peak and the peak due to the source in use were visible in the same data set. Given the 6.0 pe/keV observed for the $^{83}Kr^m$ peak as a reference, we measured the light yield of our detector as a function of energy to be constant to within 2% between 40 and 670 keV, as shown in Fig. 6. We estimate a systematic error of 1% for each point stemming from variations in the location of the $^{83}Kr^m$ peak from run to run.
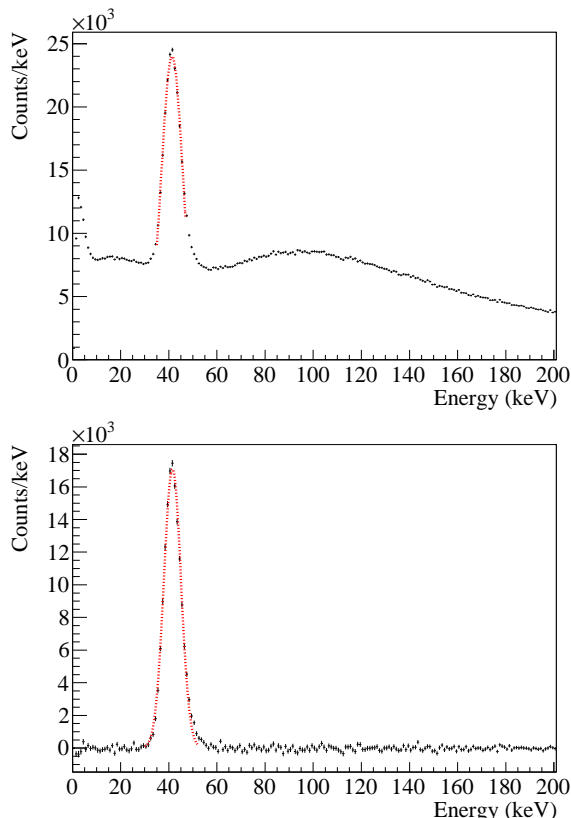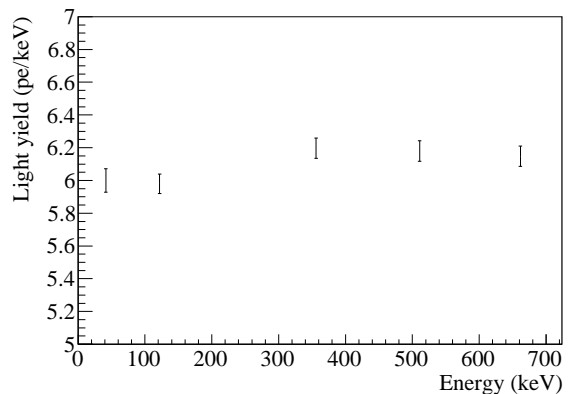

FIG. 6: Light yield versus energy in argon, referenced to the value of 6.0 pe/keV measured for the $^{83}Kr^m$ peak. There is a 1% systematic error on each point stemming from variations in the position of the $^{83}Kr^m$ peak from run to run.

FIG. 5: (Color online) Energy spectrum of $^{83}Kr^m$ runs in argon, with (bottom) and without (top) a background subtraction. The light yield is 6.0 pe/keV and the resolution is 8.2% (σ/E) at 41.5 keV.

Figures 7 and 8 show the $^{83}Kr^m$ rate as a function of time from the start and stop times of the fill respectively. While filling, the krypton rate slowly rises before reaching a steady state at 171 s^{-1}. Given the roughly 100 nCi activity of the Rb in the $^{83}Kr^m$ generator, about 6% of all $^{83}Kr^m$ atoms created reach the active volume at steady state in the active mode. The active volume makes up about 10% of the entire volume of the cell, suggesting that more than half of the $^{83}Kr^m$ atoms produced in the trap reach the liquid. Therefore, less than half of the $^{83}Kr^m$ atoms are freezing out on the detector sur-

faces. As krypton binds more efficiently to charcoal than argon, it is also likely that some fraction of the krypton is entering the charcoal trap and freezing onto the charcoal, further reducing the amount frozen to detector walls. After stopping the fill and allowing an hour for the detector to settle, we observed the $^{83}Kr^m$ to decay with a fitted half-life of (1.82 ± 0.02) hours, consistent with the reported half-life of (1.83 ± 0.02) hours.

Figure 9 shows the rate at the $^{83}Kr^m$ peak for a second run, as well as the mean value of a Gaussian fit to the asymmetry parameter, A, between 30 and 50 keV and between 50 and 100 keV. The error bars from the fit are too small to be seen on the plot. Initially, the asymmetry parameter has a slight offset due to a relative difference in the efficiency of the PMTs. As $^{83}Kr^m$ begins to enter the active region, the rate around 41.5 keV begins to increase. At the same time, the mean value of A in that region also increases, while it remains unchanged in a different energy band. We interpret this data to suggest that because the liquid enters the stainless steel vessel from the top, the $^{83}Kr^m$ first appears at the top of the active volume, causing an increase in the observed asymmetry parameter that is not seen in a different energy band. As the run continues, the $^{83}Kr^m$ fills out the entire active volume, and the asymmetry parameter returns to its usual value. Therefore, one could potentially use $^{83}Kr^m$ atoms as a tracer to understand fluid flows and mixing rates in the detector.

We performed one run in the passive filling mode, where the gas flow did not directly pass through the trap. Fig. 10 shows the rate as a function of time from beginning the fill. About one tenth the amount of krypton entered the active region as compared to the active mode, or 0.6% of all $^{83}Kr^m$ produced in the generator.

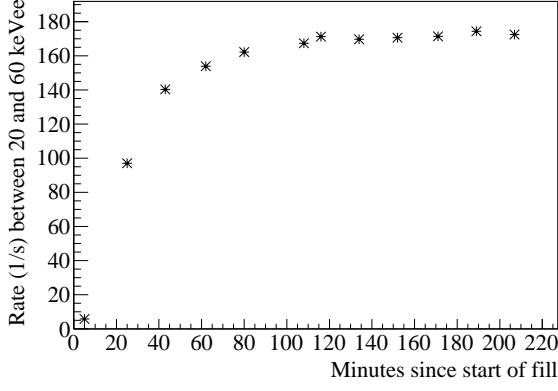FIG. 7: Rate of ^{83}Kr^{m} events in argon as a function of time from the beginning of a fill. The rate reaches a steady state at 170 s^{-1}.
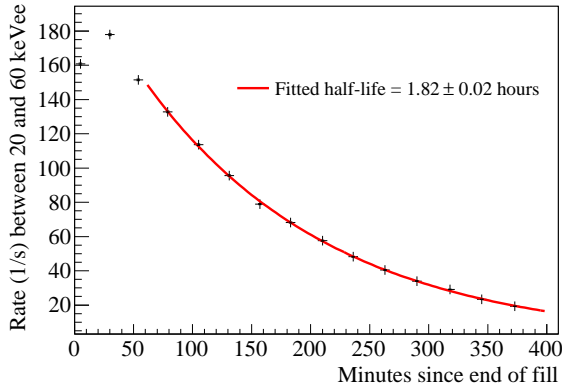

FIG. 8: (Color online) Rate of ^{83}Kr^{m} events in argon as a function of time from ending a fill. The rate decays with a fitted half-life of (1.82 ± 0.02) hours, consistent with the reported value of (1.83 ± 0.02) hours.

FIG. 9: (Color online) The top panel shows the rate of ^{83}Kr^{m} events in argon as a function of time from the beginning of the fill. The bottom panel shows the mean value of the asymmetry parameter, A, in argon during the same fill. The ^{83}Kr^{m} initially appears at the top of the detector, temporarily raising A, before filling the whole active region as discussed in the text.

B. Liquid neon

We performed one run in liquid neon in active filling mode. As mentioned in the previous section, the trigger threshold was very low and many of the observed events were low threshold noise events. While the background can still be effectively subtracted, the trigger rate is dominated by these backgrounds and the ^{83}Kr^{m} statistics are not nearly as good as for the argon runs. Even so, a clear peak appears in liquid neon at the full energy of the ^{83}Kr^{m} decay, as shown in Fig. 11. We recorded a light yield of (1.45 ± 0.2) pe/keV in the bottom PMT. From the average A value determined in argon from all runs, we determine the top tube is 6% more efficient than the bottom tube. Using the measured efficiency, we extrapolate the total light yield in liquid neon from both tubes to be (3.0 ± 0.3) pe/keV. The error is mainly due to uncertainty in the single photoelectron response of the bottom PMT. There is some error introduced by the extrapolation to the second tube, as the relative efficiency
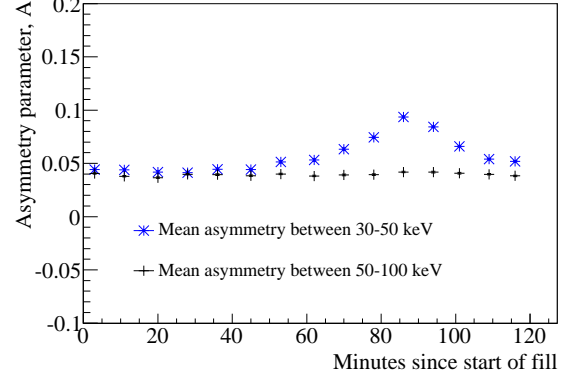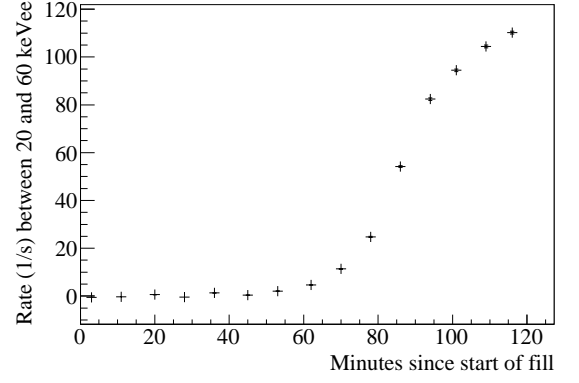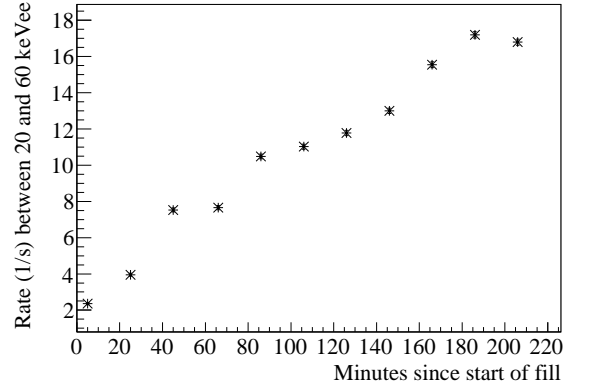

FIG. 10: Rate of ^{83}Kr^{m} events in argon as a function of time from the beginning of the fill when running in passive mode. In this mode, the rate of ^{83}Kr^{m} is 10% that observed for the active mode.

of the tubes may change between 85 K and 25 K, but this is likely to be smaller than the error already present in the determination of the single photoelectron response.

The energy resolution at 41.5 keV in liquid neon was 19% (σ/E), or $2 \times \sqrt{<N_{pe}>}$. Fig. 12 shows the decay of $^{83}Kr^m$ in the liquid after stopping the fill. We again wait one hour for liquid to stop filling the detector before observing a fitted half-life of (1.16 ± 0.56) hours. Because no counter was available during the neon run, we cannot estimate the efficiency with which $^{83}Kr^m$ atoms entered the liquid neon volume.

FIG. 12: (Color online) Rate in arbitrary units of $^{83}Kr^m$ in neon as a function of time from the end of a fill. The rate decays with a fitted half-life of (1.16 ± 0.56) hours, consistent with the value in the literature.

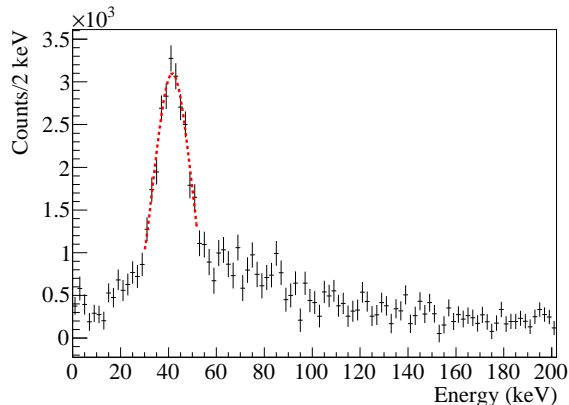FIG. 11: (Color online) Energy spectrum of a background subtracted $^{83}Kr^m$ run in neon. As discussed in the text, the extrapolated light yield is (3.0 ± 0.3) pe/keV and the resolution is 19% (σ/E) at 41.5 keV.
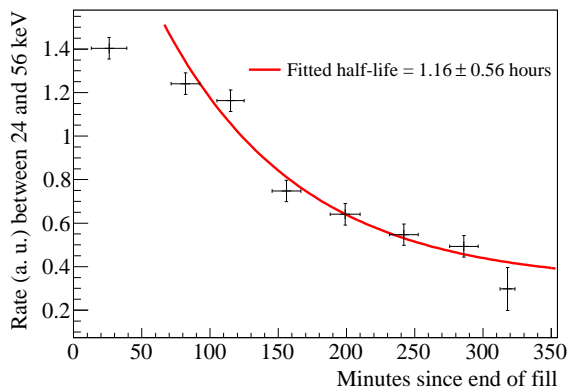

IV. DISCUSSION

The results discussed here show that $^{83}Kr^m$ is readily introduced into both liquid argon and liquid neon volumes and could serve as a useful calibration to characterize the scintillation response of argon and neon detectors at low energies. While some $^{83}Kr^m$ may be freezing onto the walls, enough atoms reach the central volume to be clearly observed. A detector with x-y position reconstruction could potentially observe $^{83}Kr^m$ atoms frozen to the walls as an exterior ring of activity in the detector. The current design for MiniCLEAN calls for a continuous purification loop, and a ^{83}Rb trap could be easily included in that design. Alternatively, it appears possible to run without directly flowing gas through the trap, although this mode is less efficient.

In addition, the asymmetry results show that it might be possible to spatially resolve krypton atoms as they enter the detector, providing a handle on flow, mixing and the spatial resolution of a large detector.

[1] J. Angle, E. Aprile, F. Arneodo, L. Baudis, A. Bernstein, A. Bolozdynya, P. Brusov, L. C. C. Coelho, C. E. Dahl, L. DeViveiros, et al., Phys. Rev. Lett. **100**, 021303 (2008).

[2] G. Alner, H. Araujo, A. Bewick, S. Burgos, M. Carson, J. Davies, E. Daw, J. Dawson, J. Forbes, and T. Gamble, Nucl. Instrum. Methods Phys. Res., Sect. A **555**, 173 (2005).

[3] V. N. Lebedenko, H. M. Araújo, E. J. Barnes, A. Bewick, R. Cashmore, V. Chepel, A. Currie, D. Davidge, J. Dawson, T. Durkin, et al., Phys. Rev. D **80**, 052010 (pages 14) (2009).

[4] R. Brunetti, E. Calligarich, M. Cambiaghi, F. Carbonara, A. Cocco, C. De Vecchi, R. Dolfini, A. Ereditato, G. Fiorillo, and L. Grandi, New Astron. Rev. **49**, 265 (2005).

[5] D. N. McKinsey and J. M. Doyle, J. Low Temp. Phys. **118**, 153 (2000).

[6] M. G. Boulay and A. Hime, Astropart. Phys. **25**, 179

(2006).

[7] *The Mini-CLEAN experiment*, vol. 173 (2007), ISSN 0920-5632, proceedings of the 7th UCLA Symposium on Sources and Detection of Dark Matter and Dark Energy in the Universe.

[8] K. Ni, R. Hasty, T. Wongjirad, L. Kastens, A. Manzur, and D. McKinsey, Nucl. Instrum. Methods Phys. Res., Sect. A **582**, 569 (2007), ISSN 0168-9002.

[9] KATRIN Collaboration, arXiv.org:0109033v1 (2001).

[10] D. Venos, A. Spalek, O. Lebeda, and M. Fiser, Appl Radiat Isot **63**, 323 (2005), ISSN 0969-8043.

[11] D. Venos, O. Dragoun, A. Spalek, and M. Vobeck, Nucl. Instrum. Methods Phys. Res., Sect. A **560**, 352 (2006), ISSN 0168-9002.

[12] S. C. Wu, Nuclear Data Sheets **92**, 893 (2001), ISSN 0090-3752.

[13] L. W. Kastens, S. B. Cahn, A. Manzur, and D. N. McKinsey, arXiv.org:0905.1766v1 (2009), accepted to Phys. Rev. C.

[14] A. Manalaysay, T. Marrodan Undagoitia, A. Askin, L. Baudis, A. Behrens, A. Kish, O. Lebeda, and D. Venos, arXiv.org:0908.0616v1 (2009).

[15] W. H. Lippincott, K. J. Coakley, D. Gastler, A. Hime, E. Kearns, D. N. McKinsey, J. A. Nikkel, and L. C. Stonehill, Phys. Rev. C **78**, 035801 (2008).

[16] D. N. McKinsey, C. R. Brome, J. S. Butterworth, R. Golub, K. Habicht, P. R. Huffman, S. K. Lamoreaux, C. E. H. Mattoni, and J. M. Doyle, Nucl. Instrum. Methods Phys. Res., Sect. B **132**, 351 (1997).

[17] J. A. Nikkel, R. Hasty, W. H. Lippincott, and D. N. McKinsey, Astropart. Phys. **29**, 161 (2008).

[18] W. H. Lippincott, D. N. McKinsey, J. A. Nikkel, D. Gastler, E. Kearns, S. B. Cahn, and Y. Shin, Phys. Rev. C (2010), to be submitted.